



PERGAMON

Available online at [www.sciencedirect.com](http://www.sciencedirect.com)

SCIENCE @ DIRECT®

Polyhedron 22 (2003) 2297–2299



POLYHEDRON

[www.elsevier.com/locate/poly](http://www.elsevier.com/locate/poly)

# Superexchange interaction enhanced through spin delocalisation in $\text{Rb}_2\text{FeBr}_5 \cdot \text{H}_2\text{O}$ as studied by polarised neutron diffraction

Javier Campo<sup>a,b,\*</sup>, Javier Luzón<sup>b</sup>, Fernando Palacio<sup>a</sup>, Angel Millán<sup>a</sup>,  
Garry J. McIntyre<sup>b</sup>

<sup>a</sup> Instituto de Ciencia de Materiales de Aragón, CSIC-Universidad de Zaragoza, C/Pedro Cerbuna 12, Zaragoza 50009, Spain

<sup>b</sup> Institut Laue Langevin, 6 rue Jules Horowitz, 38042 Grenoble Cedex 9, France

Received 7 October 2002; accepted 29 October 2002

## Abstract

Polarised neutron diffraction experiments on crystals of  $\text{Rb}_2\text{FeBr}_5 \cdot \text{H}_2\text{O}$  are reported. Experimental magnetic structure factors were analysed using a multipolar model for the magnetisation density on the iron and ligand atoms. Our results indicate that there exists an important spin transfer of 20% from the iron to the ligands. Also, a small asphericity is observed on Fe(III) ion due to the presence of the ligands. The hydrogen bridge, in the superexchange pathway  $\text{Fe}-\text{Br} \cdots \text{H}-\text{O}-\text{Fe}$ , seems to favour the spin-density transfer from the iron through bromine, thus enhancing the magnetic interaction.

© 2003 Elsevier Science Ltd. All rights reserved.

**Keywords:** Spin density; Covalent spin delocalisation; Superexchange magnetic interaction

## 1. Introduction

Crystals of  $\text{A}_2\text{FeX}_5 \cdot \text{H}_2\text{O}$ , where  $\text{A} = \text{K}, \text{Rb}$  and  $\text{X} = \text{Cl}, \text{Br}$ , contain discrete  $[\text{FeX}_5(\text{H}_2\text{O})]^{2-}$  octahedra which are connected by a network of hydrogen bonds. Compounds of this series all order as 3d-Heisenberg  $S = 5/2$  antiferromagnets [1]. Several exhaustive discussions of the superexchange pathways, and the way they affect magnetic properties, have appeared [2–4]. The essential feature is that there are no  $\mu$ -bridging groups, such as  $\text{Fe}-\text{O}-\text{Fe}$  or  $\text{Fe}-\text{X}-\text{Fe}$  linking the metal ions. All superexchange pathways are of the type  $\text{Fe}-\text{X} \cdots \text{X}-\text{Fe}$ ,  $\text{Fe}-\text{X} \cdots \text{H}-\text{O}-\text{Fe}$  or variants. The presence of hydrogen bonds seems to play an important role in the enhancement of the magnetic interactions. Interestingly enough, besides such relatively long pathways, where distances between neighbour Fe ions can be as large as 6.752 Å, the ordering temperatures are remarkably high,

e.g.  $T_N = 14.06$  and 22.9 K for  $\text{K}_2\text{FeCl}_5 \cdot \text{H}_2\text{O}$  and  $\text{Rb}_2\text{FeBr}_5 \cdot \text{H}_2\text{O}$ , respectively. This is indicative of a quite efficient propagation of the magnetic interactions.

Neutron powder diffraction experiments performed at 1.5 K on  $\text{K}_2\text{FeCl}_5 \cdot \text{H}_2\text{O}$  and  $\text{Rb}_2\text{FeCl}_5 \cdot \text{H}_2\text{O}$  [5,12] showed that the magnetic moment found in Fe ions for each sublattice is  $3.9(1)\mu_B$  and  $4.06(5)\mu_B$  for K and Rb compounds, respectively. These values are far below the  $5\mu_B$  expected for the saturated magnetic moment of  $\text{Fe}^{3+}$ . Spin delocalisation due to covalence in  $\text{Fe}-\text{X}$  and  $\text{Fe}-\text{O}$  bonds is the most likely origin of the moment reduction at Fe sites.

In order to explore such hypothesis, we have currently undertaken the examination of the magnetisation density by polarised neutron diffraction (PND) techniques across the archetypal series  $\text{A}_2\text{FeX}_5 \cdot \text{H}_2\text{O}$ . The aim is to obtain detailed experimental information of the spatial distribution of the unpaired spin density. Such studies will allow us to elucidate how the spin delocalisation, due to covalence effects, enhances the superexchange mechanism and consequently the propagation of the magnetic interactions.

In this contribution, we present the first results of PND obtained for  $\text{Rb}_2\text{FeBr}_5 \cdot \text{H}_2\text{O}$  compound.

\* Corresponding author. Present address: Instituto de Ciencia de Materiales de Aragón, CSIC-Universidad de Zaragoza, C/Pedro Cerbuna 12, Zaragoza 50009, Spain. Tel.: +34-976-76-27-42; fax: +34-976-76-12-29.

E-mail address: [jcampo@unizar.es](mailto:jcampo@unizar.es) (J. Campo).

## 2. Experimental

Experiments have been performed on a single crystal (about  $4 \times 3 \times 1 \text{ mm}^3$  in volume) of  $\text{Rb}_2\text{FeBr}_5 \cdot \text{H}_2\text{O}$  which was grown from solution following standard [1]. The crystal structure has been determined previously at room temperature by X-ray diffraction and at low temperature by powder neutron diffraction on deuterated samples [5,12]. The compound is orthorhombic (*Pnma*) with cell parameters 14.254, 10.2898 and 7.3746 Å at 30 K. The unit cell is composed of four  $\text{Fe}^{3+}$  cations in octahedral coordination with five bromine atoms and the oxygen atom of the water molecule. In order to obtain the crystal structure of  $\text{Rb}_2\text{FeBr}_5 \cdot \text{H}_2\text{O}$  at low temperature, and to determine the degree of extinction and multiple scattering in the particular crystal used in the polarised neutron experiment, an unpolarised neutron diffraction study was made on the four-circle diffractometer D10 at the Institut Laue Langevin (ILL), working at a wavelength of 1.25940 Å and at a temperature of 30 K. This temperature is considered close to  $T_N$  and yet safe enough in the paramagnetic region as to avoid short-range antiferromagnetic interactions. PND experiment was performed on the same crystal and at the same temperature on D23 lifting-counter-diffractometer at ILL. A pyrolytic graphite [0 0 2] crystal and a Heusler [1 1 1] polariser were used to monochromatise the incoming neutron beam at a wavelength of 1.329 Å and with a polarisation of 0.9479. A flipper with 98% efficiency reversed the polarisation between parallel and anti-parallel to the vertical magnetic field of 5.5 T applied to the sample to yield the magnetic flipping ratio for each reflection.  $\text{Rb}_2\text{FeBr}_5 \cdot \text{H}_2\text{O}$  crystal was mounted in two different orientations relative to the applied magnetic field. 137 reflections were measured with the [1 0 0] crystal axis parallel to the field and 189 with the [0 0 1] axis parallel. Absorption, extinction, Lorentz geometrical and multiple scattering corrections were applied to the measured intensities (D10) and flipping ratios (D23), where appropriate. Programs from CCSL suite [6] and MOLLY program [7,8] were employed to analyse the data. Since we were interested in the study of the hydrogen bonds effects in the superexchange pathways, a non-deuterated sample was used in the experiments.

## 3. Results and discussion

The crystal structure determined from the non-polarised neutron data taken from our non-deuterated single crystal of  $\text{Rb}_2\text{FeBr}_5 \cdot \text{H}_2\text{O}$  is in good agreement with that of the published [5,12]. In Table 1, structural parameters relevant to the spin-density study are listed. Full details of the refinement will be published elsewhere. In Fig. 1, the crystal structure, showing the

Table 1  
Spin-density population normalised to  $5\mu_B$  per octahedron of  $[\text{FeBr}_5(\text{H}_2\text{O})]^{2-}$ , relevant distances from Fe to ligands and structural parameters

	Population ( $\mu_B$ )	Distance to Fe (Å)	S.G. 62, <i>Pnma</i>	
Fe	3.973(2)	–	<i>a</i> (Å)	14.254
Br1	0.227(3)	2.478	<i>b</i> (Å)	10.2898
Br2	0.176(3)	2.512	<i>c</i> (Å)	7.3746
Br3	0.167(4)	2.549	<i>Z</i>	4
Br4	0.195(3)	2.542	<i>T</i> (K)	30
O	0.064(3)	2.108	<i>H</i> (T)	5.5

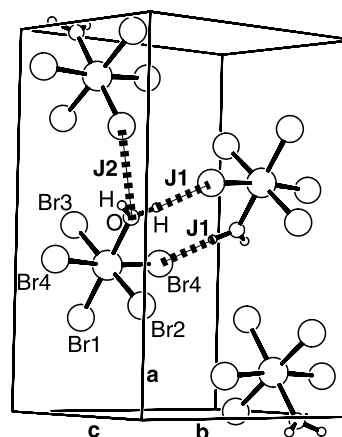


Fig. 1. Unit cell representation of  $\text{Rb}_2\text{FeBr}_5 \cdot \text{H}_2\text{O}$  with the rubidium atoms omitted for clarity. The dashed lines indicate  $J_1$  and  $J_2$  magnetic interaction pathways.

coordination octahedra of the iron atom and the strongest superexchange pathways between neighbour irons, is depicted. For clarity the rubidium atoms are omitted.

The spin-density distribution in the unit cell determined from the magnetic structure factors has been analysed in terms of a multipolar model. Due to the fact that the experiment has been done at relatively high temperature (30 K), the system magnetisation is not in the ideal condition of saturation and therefore it is difficult to extract the magnetic structure factors with high precision. To analyse the data with the minimum number of free parameters, we have considered a simplified model. Iron, to first approximation, has a spherical distribution ( ${}^6A_1:t_{2g}^3e_g^2$ ) and we will consider that the effect of the ligands only decreases the iron spin-density symmetry to  $C_4$ , where the symmetry axis is given by Br1–Fe–O line, instead of the real lower crystallographic symmetry (a mirror plane). Therefore, the iron spin density has been modelled by a hexadecapolar expansion preserving  $C_4$  symmetry. For the ligands, monopolar contributions have been assumed in our analysis. The hydrogen and rubidium spin populations were below the experimental accuracy and were not included in the final model. The values of the

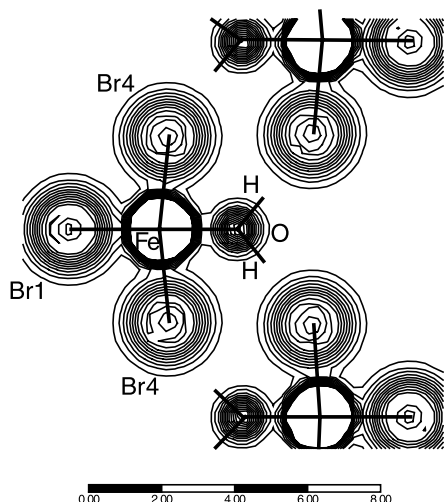


Fig. 2. Projection of the spin-density reconstruction in the plane containing Fe–X···H–O–Fe superexchange pathway. Contour levels correspond to steps of  $0.01\mu_B \text{ \AA}^{-2}$ . Total density has been normalised to  $5\mu_B$  per octahedron.

spin population, normalised to  $5\mu_B$  per octahedron, refined from this model are also listed in Table 1. The goodness-of-fit parameter  $\chi^2$  was 1.98 for the final fit. As expected, the largest spin population is found on the iron ( $3.973(2)\mu_B$ ). Moreover, a significant spin delocalisation from iron through the ligands is also observed. For example, spin populations of  $0.195(3)\mu_B$  and  $0.226(3)\mu_B$  are fitted on Br4 and Br1, respectively. Spin delocalisation effects have been observed before in other coordination compounds of 3d metal ions [9,10], but this phenomenon is very efficient in  $[\text{FeBr}_5(\text{H}_2\text{O})]^{2-}$  because it fulfils all the conditions favouring spin delocalisation due to covalence in this type of compounds [11]; it has the highest possible spin value ( $S = 5/2$ ), it has half-filled  $e_g$  orbitals allowing the spin transfer through  $\sigma$  molecular orbitals, and it is a trivalent ion.

The shorter the Fe–Br distance, the higher is observed the spin population in the bromine atom except for the one belonging to the hydrogen bridge which has  $0.195(3)\mu_B$  spin population although its distance to Fe is not the shortest one. The hydrogen bridge seems to favour the spin delocalisation from the iron atom through the ligand.

A projection of the spin-density reconstruction in the plane containing Fe–X···H–O–Fe superexchange pathway is shown in Fig. 2. This superexchange pathway, in the isomorphous  $\text{K}_2\text{FeCl}_5 \cdot \text{H}_2\text{O}$ , has the most intense magnetic coupling constant ( $J_1 = -0.184$  meV: O–H–Cl distance equal to  $3.106 \text{ \AA}$ ), and it is an order of

magnitude stronger than the second one ( $J_2 = 0.016$  meV: O–Cl distance equal to  $3.278 \text{ \AA}$ ) [4].  $J_1$  and  $J_2$  magnetic interaction constants are shown in Fig. 1. The other superexchange couplings are via two bromine atoms with Br–Br distances around  $3.9 \text{ \AA}$ . In Fig. 2, we can also observe a slight compression of the sphericity of the iron spin density in the direction of Fe–O bond because oxygen in the water molecule is less covalent than the bromine atoms.

In the superexchange mechanism [11], the magnetic orbitals are not totally localised in the magnetic atoms but also have a contribution of the ligand atomic orbitals. This delocalisation of the magnetic orbitals allows their overlap and, consequently, favours the magnetic interaction. In the compound studied, we have observed that the magnetic orbitals include an important component from ligand atomic orbitals, which explains the relatively high ordering temperature.

## Acknowledgements

We would like to thank CICYT (grant MAT2000-1388-C03-03) for financial support. The Institut Laue Langevin and the Centre d'Etudes Nucléaires de Grenoble are acknowledged for the allocation of neutron beam time on the instruments D10 and D23. Some of us (J.C., J.L. and F.P.) wish to dedicate this paper to Prof. Domingo González on his retirement.

## References

- [1] R.L. Carlin, F. Palacio, *Coord. Chem. Rev.* 65 (1985) 141.
- [2] J.A. Puertolas, R. Navarro, F. Palacio, J. Bartolome, D. Gonzalez, R.L. Carlin, *Phys. Rev. B* 26 (1982) 395.
- [3] J.A. Puertolas, R. Navarro, F. Palacio, J. Bartolome, D. Gonzalez, R.L. Carlin, *Phys. Rev. B* 31 (1985) 516.
- [4] J. Campo, F. Palacio, C.C. Becerra, A.R. Wildes, L.P. Regnault, J.E. Lorenzo-Díaz, *J. Magn. Magn. Mater.* 261 (2001) 479.
- [5] R.L. Carlin, S.N. Bhatia, C.J. O'Connor, *J. Am. Chem. Soc.* 99 (1977) 7728.
- [6] J.C. Matthewman, P. Thompson, P.J. Brown, *J. Appl. Crystallogr.* 15 (1982) 167.
- [7] N.K. Hansen, P. Coppens, *Acta Crystallogr., Sect. A* 34 (1978) 909.
- [8] E. Ressouche, Ph.D. Thesis, University of Grenoble, Grenoble, 1991.
- [9] R.J. Deeth, B.N. Figgis, M. Ogden, *Chem. Phys.* 121 (1988) 115.
- [10] P.A. Reynolds, B.N. Figgis, *Phys. Rev. B* 42 (1990) 2536.
- [11] P.W. Anderson, in: F. Seitz, D. Turnbull (Eds.), *Solid State Physics*, vol. 4, Academic Press, New York, 1963, p. 99.
- [12] M. Gabás, F. Palacio, J. Rodríguez-Carvajal, D. Visser, *J. Phys.: Cond. Matter* 7 (1995) 4725.